J. Biol. Macromol., **4** (2) 45-56 (2004)

Review

Antibody flexibility observed in antigen binding and its subsequent signaling

Masayuki Oda

Dept. Cellular Macromolecule Chemistry, Graduate School of Agriculture, Kyoto Prefectural University, 1-5 Shimogamo Nakaragi-cho, Sakyo-ku, Kyoto 606-8522, Japan.

Received June 7, 2004; Accepted July 12, 2004

Antibodies are well-known proteins that defend against bacterial and viral infections. At the molecular level, antibodies in solution are flexible and exist in populations of different structures with different energy levels which are important for antigen binding and immunological functions. In the present post-genome era, although many three-dimensional structures of proteins, including antibodies, have been determined mainly by X-ray structural analysis, quantitative analyses of the dynamic properties of proteins are needed for correlation with the protein functions. Since protein molecules always function via binding, we have investigated the binding mechanism of antibodies and the conformational change of antibodies induced upon antigen binding, which is critical for intracellular signaling. In this article, I review several reports, including our recent results of dynamic structural analyses for antibodies. These reports strongly suggest the difficulty in interpreting snapshot pictures from static structural analyses. To detect the flexible nature of protein, the development or improvement of several techniques is also in progress. Used together, the conventional methods, such as binding thermodynamics and kinetics, can provide new information on protein flexibility. These novel findings can not only shed light on the general features of protein functions but also can be put to practical use, such as the rational design of an antibody with high antigen-binding affinity.

Keywords: antibody, antigen, binding affinity, structural flexibility, structure-function relationship

Introduction

Antibodies such as IgG and IgM have a basic four-chain structure consisting of two heavy and two light chains with two antigen binding sites, termed combining sites. The antibody structure is extensively flexible, permitting antibodies to adapt to a vast array of antigen shapes and sizes, including soluble proteins and microorganisms. It is well known that the cooperation of multiple combining sites, two for an IgG and 10 for an IgM pentamer, to multivalent antigens enhances the apparent binding affinity, termed avidity, compared with that achieved with monovalent binding. This type of cooperation among different types of antigens depends on the flexibility of the Fab arms involved in the antigen binding.

Correspondence to Masayuki Oda.
Tel & Fax: +81-75-703-5673
E-mail: oda@kpu.ac.jp

Antibodies also act as antigen receptors on B-cells (BCRs) and transmit signals resulting from antigen binding. The different mechanisms involved in the effector function induced upon antigen binding have long been debated; one mechanism is the cross-linking of adjacent BCRs by the binding of a multivalent antigen, and another is the confor-

The abbreviations used are: BCR, antigen receptor on B-cell; SPR, surface plasmon resonance; ITC, isothermal titration calorimetry; K_a, equilibrium association constant: ΔG, Gibbs free energy change; k_{on}, association rate constant; k_{off}, dissociation rate constant; ΔH, enthalpy change; ΔS, entropy change; NP, (4-hydroxy-3-nitrophenyl) acetyl; HEL, hen egg lysozyme; OVA, ovalbumin; BSA, bovine serum albumin; CGG, chicken γ-globulin; NP-Cap, NP-ε-aminocaproic acid; ELISA, enzyme-linked immunosorbent assay; SpG, streptococcal protein G; SpA: staphylococcal protein A; ΔC_p, heat capacity change; CDR, complementarity-determining region

mational change in the antibody. Although many crystal structures of liganded and unliganded Fab or Fv fragments of antibodies have been determined, the central question about the relationship between effector function and conformational change remains unanswered, mainly because of the difficulty in detecting the fine and dynamic conformational differences.

Not only a global conformational change but also a site-specific change occurs in an antibody upon antigen binding. We have recently shown that kinetic and thermodynamic analyses are powerful tools to detect subtle conforamational changes and reveal the flexible nature of an antibody. In these investigations, we have mainly used the Biacore system, which utilizes surface plasmon resonance (SPR) as a means of detection, and isothermal titration calorimetry (ITC), which can detect heat in the binding of biological interactions with high sensitivity. Both SPR biosensors and ITC have been widely used to measure biomolecular interactions, not only for determining equilibrium association constant (K_a) and Gibbs free energy change (ΔG) but also for binding kinetic rate constants, association rate (k_{on}) and dissociation rate (k_{off}) constants, and thermodynamic parameters, binding enthalpy (ΔH) and entropy (ΔS) changes, respectively [1].

In this review article, I show several examples, including our recent results of dynamic structural analyses of antigen-antibody interactions, which can provide unknown features of an antibody in comparison with or in addition to static structural analyses. These results can aid in understanding the flexible nature of antibodies in antigen recognition and the implication of subsequent signaling via antibodies. In our investigations, we used a series of mouse monoclonal antibodies specific to a hapten, (4-hydroxy-3-nitrophenyl)acetyl (NP), which has been commonly used as a T-cell-dependent antigen.

Binding avidity and stoichiometry of IgG

In order to analyze the effects of antigen size and valence on antibody binding, we prepared antigens with different numbers of NPs conjugated to various proteins, such as hen egg lysozyme (HEL), ovalbumin (OVA), and bovine serum albumin (BSA) (Table 1). The monoclonal antibodies used were anti-NP IgG1s, F8, A6, B2, and C6, obtained at different stages of immunization (Table 2). In the binding experiments using SPR, an antigen or antibody was immobilized on the sensor chip surface, and another molecule, either antibody or antigen, was injected into the flow (Fig. 1). The former immobilization method is a model of bacteria or viruses interacting with soluble antibodies, and the latter is a model of BCRs interacting with soluble antigens [2].

In the method of antibody immobilization, the anti-NP antibody was captured through its Fc region on a rabbit anti-mouse Fc antibody chemically attached to the sensor chip surface. This method enabled us to determine the binding

Table 1. Sizes of carrier proteins used in the NP conjugates

protein	molecular weight (k)	surface area[a] (Å^2)
HEL	14	6.5×10^3
OVA	45	1.6×10^4
BSA	67	2.7×10^4
CGG	150	6.2×10^4
MMG	900	3.1×10^5

[a] The estimation was based on the crystal structures [61, 62]. The surface areas of BSA and CGG were assumed to be the same as those of human serum albumin and mouse IgG1 antibody [33, 63]. The surface are of MMG was assumed to be 5-fold that of mouse IgG1 antibody.

Table 2. Antigen binding affinity and avidity of anti-NP IgG1 and IgM antibodies

antibody	time after immunization (week)	$K_{a,\ affinity}$[a] (M^{-1})	$K_{a,\ avidity}$[b] (M^{-1})
F8	1	2.7×10^5	2.5×10^8
A6	1	2.5×10^6	4.5×10^8
B2	2	3.4×10^6	4.3×10^8
C6	12	3.3×10^7	4.1×10^8
A6-hCμ[c]	—	2.5×10^6	8.8×10^8

[a] The $K_{a,\ affinity}$ values for monovalent binding to NP-ε-aminocaproic acid (NP-Cap) were determined by ITC at 37°C [25].
[b] The $K_{a,\ avidity}$ values were determined from the divalent binding to higher valenced NP-BSA at 25°C.
[c] Transfectoma produced IgM pentamer, which has A6 and human Cμ at the V and C regions, respectively.

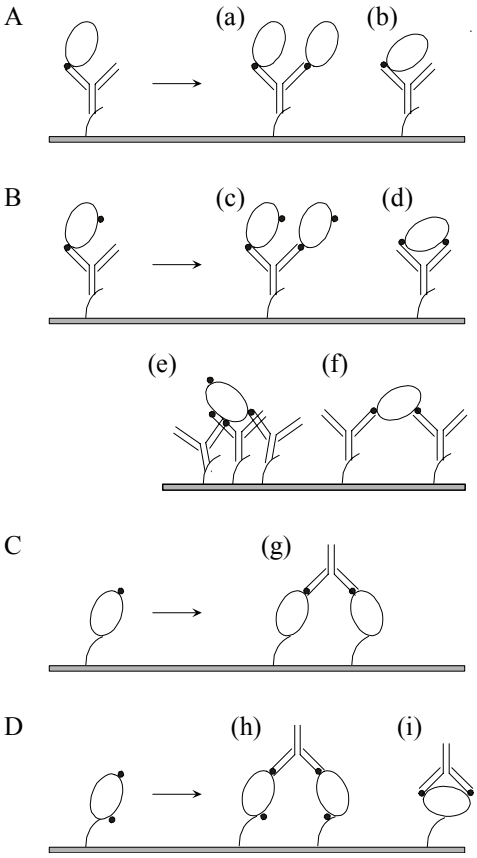

Figure 1. Schematic representation of interactions between antigen and antibody. (A) Models of interactions between monovalent antigens and immobilized antibodies. Only two antigen-antibody complexes would form with monovalent antigens. (B) Models of interactions between multivalent antigens and immobilized antibodies. (C) Models of interactions between free antibodies and immobilized monovalent antigens. (D) Models of interactions between antibodies and immobilized multivalent antigens. The closed circles and open ellipses represent haptens and carrier proteins, respectively.

stoichiometry of antigen to antibody since all of the immobilized anti-NP monoclonal antibodies could interact with antigens. It was found that the two combining sites of an antibody were able to simultaneously accommodate two NP_1-HELs as well as NP_2-HEL at a high antigen concentration, resulting in a tri-molecular complex, Ag_2Ab_1 (Figs. 1a and 1c). In contrast, NP conjugates of the larger proteins, such as OVA and BSA, formed only a di-molecular complex, Ag_1Ab_1, irrespective of the hapten valence (Figs. 1b and 1d). The variation in the binding stoichiometry with antigen size can be explained in terms of the restriction of elbow-bending flexibility within the Fab arms and hinge bending between two Fab arms. These findings are supported by the results of experiments related to binding of protein antigens, such as HEL, OVA, and BSA, to monoclonal antibodies specific to the respective proteins (Oda *et al.*, unpublished results), and the recent analysis using cryo-electron microscopy, as described below [3]. At a low concentration of multivalent antigen, the K_a values were higher than those at a high antigen concentration, suggesting that multivalent binding had occurred (Figs. 1e and 1f).

The method of antigen immobilization is useful for providing information on the binding avidity of an antibody and its correlation with monovalent binding affinity. Since the dextran layers of the Biacore sensor chip surface are mobile, the divalent binding of IgG can be classified into intermolecular and intramolecular bindings, depending on the types of immobilized antigens. When NP-HEL antigens are immobilized, intermolecular divalent binding occurs due to the small size of HEL, in addition to monovalent binding (Figs. 1g and 1h). In this case, the binding of the lower affinity antibody, F8, was not detected, while the binding of higher affinity antibodies was. These results indicate that neither the monovalent binding nor intermolecular divalent binding of F8 is under the detection limit of Biacore, probably due to the upper limit for the k_{off} value [4]. The results of the binding experiments using immobilized NP-HEL and NP-BSA surfaces indicate that the difference in avidity between intermolecular and intramolecular divalent bindings is smaller for the antibody with higher monovalent affinity. In intramolecular divalent binding with maximum avidity (Fig. 1i), the apparent binding strengths of F8, B2, A6, and C6 appeared likely to increase by approximately 1,000-, 200-, 100-, and 10-fold relative to the monovalent affinity (Table 2). These results suggest that antibodies with lower affinity can increase their binding strength to a larger extent. In addition, it should be noted that the K_a values for the maximum avidity are similar in all antibodies, which seems to be due to the ceiling avidity. It has been reported that the physiological role of somatic hypermutation is to allow antibodies to attain an affinity ceiling of $K_a \approx 10^{10}$ M^{-1} [5]. The

ceiling affinity does not seem to be responsible for the limitation of the antibody architecture because the yeast-surface-displayed antibody has been shown to have 2.1×10^{13} M^{-1} monovalent affinity [6]. Based on these results, the ceiling affinity or avidity *in vivo* maturation is considered to be enough for the immune system.

Binding avidity and stoichiometry of IgM

The secreted IgM molecule is a pentamer made up of five four-chain subunits and one J-chain, and it occurs in body fluid in the form of natural antibodies. When mice were immunized with proteins or haptenated proteins, IgM was produced as the primary antibody, followed by the production of IgG as the secondary antibody. It has been considered that an IgM pentamer uses 10 Fab arms to bind to antigens with higher avidity, which can compensate for the lower binding affinity of each combining site [7]. However, little is known about how IgM binds to smaller antigens using multiple combining sites. In order to examine how the binding avidity of IgM depends on the antigen size and epitope density, we analyzed the interactions of anti-NP IgM with antigens of different numbers of NP conjugated to various proteins, such as BSA, chicken γ-globulin (CGG), and mouse anti-dansyl monoclonal IgM, designated as MMG (Table 1) [8]. The antibodies used were an anti-NP IgG1, A6, and a chimeric anti-NP IgM pentamer, A6-hCμ, having A6 and human Cμ at the V and C regions, respectively.

The analysis of binding stoichiometry has shown that A6-hCμ binds to NP-BSA and NP-MMG with Ag_5Ab_1 and Ag_1Ab_1 complexes, respectively. The model in which one NP-BSA molecule binds to one monomer subunit of IgM is in accordance with the results for IgG, as described above. This finding suggests that IgM is unable to form a complex involved with multiple subunits, further suggesting that IgM is not flexible enough to hold a single antigen of small size, such as a "seaflower-like" configuration. In contrast, with an antigen larger than IgM, five IgM subunits would participate in binding to a single antigen molecule. It is interesting to reconsider the previous reports that electron microscopy showed that an antigen-bound IgM has a "crab-like" configuration. Such a conformational change would be necessary for activation of the complement cascade [10].

The K_a values of A6-hCμ were always higher than those of A6 on comparing their binding with NP-MMG of the same NP valence, although the difference became smaller for the higher valenced NP-MMG. These results indicate that IgM is superior to IgG in interactions with antigens of a larger size and lower hapten density. The highest K_a value of A6-hCμ for NP-conjugates was 8.8×10^8 M^{-1} (Table 2). Again, this should be the ceiling avidity. Assuming that the combining sites of IgM are freely accessible to epitopes on the antigen molecule without any steric hindrance, the apparent K_a value can be expressed as $K_a = (K_1)^{10}$, where K_1 is an intrinsic association constant of each combining site. However, in practice, the maximum K_a value of IgM is much lower than the theoretically predicted value, which is the same as that of IgG, suggesting that the respective combining sites can not act independently each other, and the binding of one Fab arm provides a negative influence on the binding of other.

A similar analysis was recently reported which shed light on the correlation between the antigen binding ability and segmental flexibility of an antibody [11]. In this article, the binding properties of the IgM monomer and IgD to the antigens of different epitope densities are compared, and correlated with the respective flexibilities determined by electron microscopy. IgD is the major component of BCR, coexpressed with IgM on the surface of naïve B-cells, and has long and Cys-free hinge regions which give IgD a more flexible nature than IgM. It has been shown that an IgM monomer forms a more stable complex with an antigen of high epitope density due to the small loss of entropy, while IgD has an advantage for the binding to an antigen of low epitope density due to its flexibility. The same group also reported the rank orders of the mean Fab-Fab angles and the hinge-fold flexibility function of human subclasses; the former rank order is IgD, IgE > IgG3 > IgG4 > IgG2 > IgG1 > IgA2 > IgM, and the latter rank order is IgD > IgM > IgG3 > IgG1 > IgG4 > IgA2, IgE > IgG2 [11-13].

Application for the detection of different affinities of antibodies

We have developed simple methods using enzyme-linked immunosorbent assay (ELISA) and flow cytometry to estimate the relative affinities of antibodies and BCRs based on antibody affinity and avidity, as described above [14]. In the detection system, the binding of NP-specific BCRs to NP-BSA conjugated with biotin molecules is observed using peroxidase-labeled goat anti-mouse antibodies in ELISA and streptavidin-*R*-phycoerythrin by flow cytometry. At a concentration of 100 ng/ml of antibodies in ELISA, the binding ratio of lower valenced NP-BSA per higher valenced NP-BSA was less than 0.1 for lower affinity anti-NP antibodies, such as N1G9 and A6, while it was close to 1 for higher affinity antibodies, such as B2 and C6 (Table 3). Similarly, at a concentration of 10^{-8} M of antigens in flow cytometry analysis, the binding of lower valenced NP-BSA to lower affinity BCRs on hybridomas and transfectants was observed to a small extent only, while that to higher affinity BCRs was detected with a mean fluorescence intensity similar to the binding of higher valenced NP-BSA. These results are in good agreement with those obtained by SPR and indicate the possibility for practical measurements of the antibody affinity, including that of BCR on the cell surface. Furthermore, our reagent and method can be useful to identify the memory B-cell population at different stages of affinity maturation.

Table 3. Comparisons of the relative affinities analyzed by different methods

antibody	ELISA	FACS	SPR
N1G9	0.02	0.02	0.12
A6	0.12	0.07	0.14
B2	1.17	0.73	0.64
C6	1.48	1.16	0.72

The relative affinity is shown as the ratio of $NP_{0.5}$-BSA-bio_{21} to $NP_{7.4}$-BSA-bio_{21}.

Conformational change induced by antigen binding

We have addressed the question of whether antigen binding induces a conformational change in the constant domain of an antibody using streptococcal protein G (SpG) or staphylococcal protein A (SpA) as probes since these proteins are known to bind to IgG domains such as C_H1 and the C_H2-C_H3 interface [15, 16]. The results of binding experiments using SPR and ITC between the probes and anti-NP monoclonal antibodies, IgG1 and IgG2b subclasses, in the presence or absence of an antigen show that antigen binding brought about a 30-60% decrease in affinity with the probes as shown in Table 4 [17]. In addition, the antigen binding accelerated the dissociation of the antibody from the complexes with the probes. Similar results were also observed with anti-HEL monoclonal antibodies, suggesting that our observations are not specific to anti-NP monoclonal antibodies. Since small NP antigens, such as NP-ε-aminocaproic acid (NP-Cap) and NP-Gly, were used in this experiment, the antigens could cause no steric hindrance of the interaction between antibodies and the probes. In addition, the presence of an antigen resulted in no aggregation of antibodies. These results confirm that the decreased binding affinity for the probes in the presence of an antigen is due to the conformational change in binding sites for the probes, which are distant from the combining sites.

A controversy has long existed over whether antigen binding induces a conformational change in C_H domains and results in subsequent signaling by an allosteric mechanism, such as the activation of the complement cascade or IgG transport through the membrane [10, 18, 19]. Nanosecond fluorescence polarization studies of anti-dansyl monoclonal antibodies have shown that the rank orders of mean rotational correlation times of mouse subclasses are IgG2b > IgG2a > IgG1 > IgE, and they are correlated with the ability to complement fixation [20]. These results indicate the transmission of conformational change from the Fab to the Fc region, which changes to the favorable conformation for complement fixation. In addition, it has been shown that B-cell lines or transfectants can present monovalent antigens to T-cells, indicating that the cross-linking of BCRs is not required for antigen presentation by B-cells and is still necessary for signal 1 in the differentiation of naïve B-cells to antibody-forming cells [21, 22]. We have succeeded in detecting the fine conformational change in C_H do-

Table 4. K_a values of anti-NP IgG1 antibodies for the interactions with the immobilized SpG-C2 and SpA-B in the absence or presence of NP-Cap

antibody	SpG-C2 [a] –antigen (M^{-1})	+antigen (M^{-1})	ratio [b]	SpA-B [a] –antigen (M^{-1})	+antigen (M^{-1})	ratio [b]
F8 (IgG1)	8.3×10^6	3.8×10^6	0.46	7.2×10^6	4.8×10^6	0.67
B2 (IgG1)	5.4×10^6	1.7×10^6	0.31	7.4×10^6	2.1×10^6	0.28
C6 (IgG1)	3.3×10^6	1.7×10^6	0.52	4.3×10^6	1.4×10^6	0.33
6L1 (IgG2b)	2.9×10^7	1.7×10^6	0.59	1.5×10^7	6.0×10^6	0.40
9L2 (IgG2b)	2.5×10^7	1.6×10^7	0.64	1.4×10^7	6.3×10^6	0.45

Biacore experiments were carried out in PBS containing 0.005% Tween 20 at 25°C.
[a] SpG-C2 and SpA-B are the C2 domain of SpG and the B domain of SpA, respectively.
[b] The ratio was calculated by dividing the K_a value obtained in the presence of NP-Cap by that obtained in the absence of NP-Cap.

mains [17], and have further shown that a B-cell transfectant is activated by NP-protein conjugates which cannot cross-link antibodies (Oda *et al*., unpublished results). In addition, we have analyzed the interactions of IgG2a or its enzymatic fragments with SpA in the presence or absence of the hapten and shown novel features of the complex formation to support the conformational changes in the antibody constant domains upon antigen binding (Sagawa *et al*., submitted). It should be noted that Fab and $F(ab')_2$ fragments of anti-NP IgG2a antibodies bind to not only SpG but also SpA and the hapten binding weakens the interactions of $F(ab')_2$ fragments. Based on these results, we propose a new model of the antibody-SpA complex which can explain the conformational change induced by antigen binding.

Alteration of antigen recognition during affinity maturation

Affinity maturation refers to an increase in antibodies, generally observed following immunization with T-cell-dependent antigen which consists of the ongoing generation of B-cells with a mutant BCR due to the somatic hypermutation and selection of these cells on the basis of affinity. The amino acid substitution of antibodies, caused by somatic hypermutation, creates variability for antigen recognition. It has been shown that affinity of anti-NP antibodies to NP increases more than 8,000-fold with time after immunization [23].

In order to understand the mechanism of affinity maturation, thermodynamic analysis was applied to antigen-antibody interactions. Previously, using three anti-NP monoclonal antibodies; N1G9, a germline antibody; and 3B44 and 3B62, affinity matured antibodies; the magnitude of ΔH, ΔS, and heat capacity change (ΔC_p) for the binding of NP-Cap was shown to increase the corresponding binding affinity almost linearly [24]. These results suggest that a better surface complementarity was attained in the specific complex in order to obtain a higher affinity. Our recent thermodynamic analyses using more than 30 anti-NP monoclonal antibodies have shown that the ΔH and ΔS values of antibodies with higher affinity do not always increase, although the correlation between ΔH and ΔS values is almost linear, as shown in part in Table 5 [25]. This finding indicates that the architecture of the antibody, including not only the combining sites but also the framework regions, totally contributes to the increased binding affinity. The effects of protein flexibility and salvation can also make the thermodynamic origin complex. In the course of our studies, we obtained a group of anti-NP monoclonal antibodies, 9T7, 9T8, 9T10, and 9T13, 9 weeks after the immunization of C57BL/6 mice, and found them to originate from a common ancestor, judging from the nucleotide sequences [26]. It should be noted that their increased binding affinities (9T7 < 9T8 < 9T10 < 9T13) were accompanied by increased ΔS values without any significant change in enthalpy (Table 5). In addition, the kinetic measurements show that both the k_{on} and k_{off} values decreased during affinity maturation (Table 6). These results suggest that the antigen-binding mechanism of these antibodies shifts from a “induced-fit” type to a “lock-and-

key" type during antibody evolution [27]. The decreased k_{on} values of more mature antibodies provide a negative effect on affinity and are in contrast to kinetic maturation [28]. In the case of the NP-hapten system at least, antibodies undergo an increase in the K_a value by a change in both the k_{on} and k_{off} values (Table 6), and at the late stage of affinity maturation, the antigen-antibody interaction should shift from a "induced-fit" type to a "lock-and-key" type of mechanism. The affinity-maturation-dependent decreases in k_{off} values have been interpreted in terms of rigidifying mutations that stabilize favorable conformations of combining sites, while increases in k_{on} values have been interpreted in terms of kinetic selection for rapid antigen association [28-31].

Table 5. Thermodynamic parameters of the interactions between NP-Cap and anti-NP IgG1 antibodies

antibody	ΔG°	ΔH (kcal/mol)	$T\Delta S^\circ$
F8	–10.2	–13.4	–3.2
A6	–11.5	–25.6	–14.1
B2	–11.7	–18.1	–6.4
C6	–13.1	–24.2	–11.1
9T7	–13.2	–18.9	–5.7
9T8	–13.5	–19.1	–5.6
9T10	–13.7	–18.8	–5.1
9T13	–13.9	–19.1	–5.2

ITC experiments were carried out in PBS at 37°C.

Table 6. Kinetic rate constants of the interactions between NP-HEL and anti-NP IgG1 antibodies

antibody	k_{on} ($M^{-1}s^{-1}$)	k_{off} (s^{-1})	$K_{a,kin}$[a] (M^{-1})
B2	8.7×10^4	8.1×10^{-2}	1.1×10^6
C6	1.7×10^5	1.7×10^{-2}	1.0×10^7
9T7	5.5×10^5	1.3×10^{-2}	4.2×10^7
9T8	5.4×10^5	7.5×10^{-3}	7.2×10^7
9T10	1.8×10^5	2.3×10^{-3}	7.8×10^7
9T13	3.9×10^5	2.5×10^{-3}	1.7×10^8

Biacore experiments were carried out in PBS containing 0.005% Tween 20 at 25°C.
[a] The $K_{a,kin}$ values were calculated from the two kinetic rate constants, $K_{a,kin} = k_{on}/k_{off}$.

Comparison with crystal structural analyses

Two intact mouse monoclonal antibodies, IgG1 and IgG2a, were crystallized and their molecular structures determined [32, 33]. The results show that IgG1 has an angle of 115° between two Fab arms so that it exhibits a "distorted Y shape", while IgG2a has an angle of 172° so that it exhibits a "distorted T shape". Because proteins are flexible and exist in populations of different structures in general, it is natural to consider that these crystal structures are like "snapshots" within the wide spectrum of conformers that can be attained by the antibody molecule. Our method, using various antigens of different sizes and epitope densities, is a novel approach to analyze the antibody flexibility in antigen-antibody interactions [2, 8, 14].

The crystal structures of the Fab fragments of an anti-NP monoclonal antibody, N1G9, in unliganded and liganded states, are available and show major structural differences induced by antigen binding, especially in the complementarity-determining regions (CDRs) [34]. This finding suggests that an adaptation occurs in CDRs upon antigen binding, similar to other antigen-antibody complexes [35, 36]. In addition to the changes in CDRs, relatively large differences upon complex formation can also be observed in the V_H and C_H1 domains of N1G9. Although it is not yet certain whether the changes observed in the crystal structures are related to the conformational change induced by antigen binding in solution, the observed change in the C_H1 domain is of particular interest since this region was shown to be involved in SpG binding and affected by antigen binding in our investigations [17]. With respect to the influence on SpA binding in the C_H2-C_H3 region, there is no direct structural evidence that the conformational change is transmitted to the C_H2-C_H3 region through the flexible-hinge region.

In terms of affinity maturation, some structural analyses are available in which the crystal structures of germline antibodies are compared with those of the corresponding affinity-matured antibodies. Nitrophenyl phosphonate, a hapten antigen, binds to the germline antibody with significant changes in the configuration of the combining site, while the hapten binds to the matured antibody by a "lock-and-key" mechanism [37]. In the matured antibody, many of the somatic mutations reconfigure the combining sites by reorganizing networks of hydrogen-bonding,

electrostatic, and van der Waals interactions over distances of 15 Å. The improved complementarity to hapten is accompanied by the entropic restriction of residues in the combining site, which contributes to the 30,000-fold increased binding affinity. The recent structural analysis of germline and the mature antibodies specific to both polyether jeffamine and its cognate hapten N-methylmesoporphyrin provide an interesting finding of the structural plasticity of the germline antibody and the structural effects of the somatic mutations that result in increased affinity for the hapten and decreased affinity for jeffamine [38]. Significant conformational changes upon the binding of these two structurally distinct antigens are observed in this germline antibody. The effects of somatic mutations are not only the fixing of the optimal combining site for the hapten but also the introduction of the interactions that interfere with the binding of jeffamine, resulting in the antigen specificity of the matured antibody. The re-organization of the combining site in the affinity-matured antibody is also supported by the results of molecular dynamics simulations [39]. Based on these results, together with our investigations for antigen-antibody interactions in solution, at least three mechanisms can be proposed for increasing affinity by somatic mutations; 1) direct interaction with the bound antigen, 2) decreased structural flexibility of a germline antibody, and 3) reorganization of the antigen-antibody interface [40]. Through general mechanisms by the immune response, the germline antibody repertoire is expanded to multiple combining-site configurations, while somatic mutations can stabilize the configuration to interact with specific antigens, resulting in high affinity and specificity.

Protein flexibility in correlation with the energy landscape

Although the crystal structure at atomic resolution is important to understand the protein structure and the recognition mechanism between the biological molecules, there remain some problems to be considered. The obtained structure is like a snapshot, as described above, and it can be affected by unpredictable errors originating from the special packing environment within the crystals. A collection of these snapshots corresponds to the equilibrium conformation of a protein, which is critical for understanding the biological function. The determination or prediction of the functions of the encoded protein sequences, based on the three-dimensional structures, will be a major challenge in the post-genome era. The ensemble nature of protein conformations is depicted on the energy landscape of protein folding, namely the folding funnel, which covers the entire conformational space allowed for a protein [41]. This concept has been widely accepted for protein folding and is considered to apply for protein binding [42]. In solution, proteins frequently coexist in a wide range of conformations (Fig. 2). In the "lock-and-key" binding, the funnel bottom is an association of two proteins in their most populated native conformations. In "induced-fit" binding, the complex is generated by the minor population(s) of protein(s) with conformational changes, which are sometimes coupled with the local folding of a protein [43, 44].

Although the higher energy conformers as well as the lower ones are required in order to und-

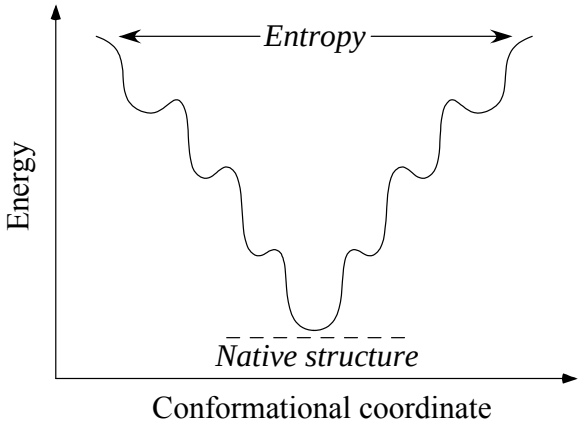

Figure 2. Schematic illustration of the energy landscape. When the energy landscape is smooth, the native protein would have small fluctuations. When the landscape is rugged, the ensemble of protein structures would include various conformations. In protein binding, "lock-and-key" and "induced-fit" types can be explained using the energy landscape, as described in the text. The landscape in "lock-and-key" binding would have few energy minima and the lowest energy bottom, separated clearly from others. In contrast, the landscape in "induced-fit" binding would have a rugged bottom with rather low barriers separating them.

erstand the mechanisms of protein folding and function, the minor population of the higher energy conformers is normally hidden behind the overwhelming population of the lower energy conformers [45]. It is difficult to detect the minor population using spectroscopic methods since even conventional NMR can only provide an averaged and single three-dimensional structure close to the crystal structure. In contrast, it should be noted that thermodynamic analysis has an advantage for detecting the total energy of all populations in solution, including not only the intra- or inter-molecular interactions but also the protein flexibility and the solvation effect. For example, our thermodynamic analyses of major histocompatibility complex class II molecules reveal the mechanisms of peptide binding and peptide exchange at acidic and neutral pHs, which are correlated with the dynamic conformational property of the protein [46-48]. These findings provide new insight into the current structural model. At the next stage, our understanding will be advanced if the thermodynamics can be classified according to each contribution of its origin and correlated with the atomic-resolution structure more quantitatively. With respect to this challenge, NMR relaxation methods have been applied for the interpretation in terms of heterogeneous partitioning between enthalpy and entropy [49, 50]. In the thermodynamics of protein folding, molecular dynamics calculations of both native and denatured proteins have shown that about 25% of the total ΔS is reflected by changes in simulated values based on the NMR-derived order parameters [51].

Future development

Cryo-electron microscopy will be one of the useful methods to detect the ensemble nature of a protein since the sample in solution is quenched to the temperature of liquid nitrogen. The structure of a neutralizing monoclonal antibody bound divalently to the human rhinovirus has revealed that the spanning distance for divalent binding is within a range of 60-140 Å [52, 53]. Recent cryo-electron microscopic tomography experiments using single-particle analysis have shown that the average value of the Fab-Fab angle of a monoclonal IgG2a antibody is approximately 110° and is distributed with a standard deviation of approximately 30° [3]. This finding is quite different from the crystal structure of the same subclass antibody, which has a “distorted T shape” [32], and demonstrates the difficulty in interpreting protein structures.

The development or improvement of other techniques to detect the flexible nature of protein is underway. One technique is multidimensional NMR spectroscopy in conjunction with variable-pressure perturbation [54]. The idea is based on the fact that the conformational order of globular protein normally decreases in parallel with its partial molar volume and the population shifts to a less-ordered conformer with increasing pressure. The same group has applied this technique to various proteins, such as HEL, prion, and the Ras-binding domain of RalGDS, and shown a good correlation with the respective protein functions. The traditional method using stopped-flow measurement is also applicable. Pre-steady-state kinetics and crystal structural analysis revealed an equilibrium between different conformers of an antibody, which generates multispecificity to different antigens [55]. It has been shown that photon-echo spectroscopy can measure the response to the electronic excitation of an antigen, fluorescein, bound to an antibody [31, 56]. This method can determine the time scale of the motions of combining sites in a range from tens of femtoseconds to nanoseconds. These flexibility analyses in comparison with germline and affinity-matured antibodies demonstrate that the antibody evolved from a flexible germline antibody into more rigid mature antibody.

With respect to the practical application of antibodies, such as humanized antibodies as drugs, many questions remain unanswered. For instance, how can antigen binding affinity, specificity, and antibody stability rationally be increased? Although the present methods of rational designs for not only antibodies but also other target molecules seem to focus only on the improvement of the binding-surface complementarity, the knowledge of global architecture is needed. It has been shown that substitution outside the combining site can increase antigen-binding affinity and alter the conformation of the combining site [26, 30, 37]. In general, conformational changes due to the protein

flexibility can cause the failure of computer models to properly identify inhibitory compounds [57]. As described above, the residues at a distance from the combining site are mutated in the antibody with femtomolar antigen-binding affinity [6]. Similarly, the residues at the joint between the V_H and C_H domains of a humanized antibody are critical for potent neutralizing activity against human IFN-γ, suggesting the importance of the antibody flexibility in an active state [58]. In addition, several reports have shown the critical residues at the V_H and V_L interface for antigen binding and antibody stability [59, 60]. In order to solve these problems, we should learn much more from nature and apply the knowledge to rational design. For example, because affinity maturation results from the repetitive generation and selection of B-cells, the structural analysis of antibodies in the process should provide new information which is applicable to the design of antibodies. With the development and improvement of techniques to detect dynamic structural and functional properties of antibodies, a new stage in the post-genome era will begin.

Acknowledgements

The author thanks to graduate students at Tokyo University of Science, Toranosuke Tobita and Takuma Sagawa, for the collaboration, and Prof. Takachika Azuma as a supervisor of our investigations presented in this review article.

References

1. Oda, M., and Nakamura, H. (2000) Thermodynamic and kinetic analyses for understanding sequence-specific DNA recognition. *Genes to Cells* **5**, 319-326.
2. Oda, M., and Azuma, T. (2000) Reevaluation of stoichiometry and affinity/avidity in interactions between anti-hapten antibodies and mono- or multi-valent antigens. *Mol. Immunol.* **37**, 1111-1122.
3. Bongini, L., Fanelli, D., Piazza, F., De Los Rios, P., Sandin, S., and Skoglund, U. (2004) Freezing immunoglobulins to see them move. *Proc. Natl. Acad. Sci. USA* **101**, 6466-6471.
4. Karllson, R. (1999) Affinity analysis of non-steady-state data obtained under mass transport limited conditions using BIAcore technology. *J. Mol. Recognit.* **12**, 285-292.
5. Foote, J., and Eisen, H. N. (1995) Kinetic and affinity limits on antibodies produced during immune responses. *Proc. Natl. Acad. Sci. USA* **92**, 1254-1256.
6. Boder, E. T., Midelfort, K. S., and Wittrup, K. D. (2000) Directed evolution of antibody fragments with monovalent femtomolar antigen-binding affinity. *Proc. Natl. Acad. Sci. USA* **97**, 10701-10705.
7. Davis, A. C., and Shulman, M. J. (1989) IgM–molecular requirements for its assembly and function. *Immunol. Today* **10**, 118-122, 127-128.
8. Tobita, T., Oda, M., and Azuma, T. (2004) Segmental flexibility and avidity of IgM in the interaction of polyvalent antigens. *Mol. Immunol.* **40**, 803-811.
9. Feinstein, A., and Munn, E. A. (1969) Conformation of the free and antigen-bound IgM antibody molecules. *Nature* **224**, 1307-1309.
10. Brown, J. C., and Koshland, M. E. (1975) Activation of antibody Fc function by antigen-induced conformational changes. *Proc. Natl. Acad. Sci. USA* **72**, 5111-5115.
11. Løset, G. A., Roux, K. H., Zhu, P., Michaelsen, T. E., and Sandlie, I. (2004) Differential segmental flexibility and reach dictate the antigen binding mode of chimeric IgD and IgM: implications for the function of the B cell receptor. *J. Immunol.* **172**, 2925-2934.
12. Roux, K. H., Strelets, L., and Michaelsen, T. E. (1997) Flexibility of human IgG subclasses. *J. Immunol.* **159**, 3372-3382.
13. Roux, K. H, Strelets, L., Brekke, O. H., Sandlie, I., and Michaelsen, T. E. (1998) Comparisons of the ability of human IgG3 hinge mutants, IgM, IgE, and IgA2, to form small immune complexes: a role for flexibility and geometry. *J. Immunol.* **161**, 4083-4090.
14. Shimizu, T., Oda, M., and Azuma, T. (2003) Estimation of the relative affinity of B cell receptor by flow cytometry. *J. Immunol. Methods* **276**, 33-44.
15. Deisenhofer, J. (1981) Crystallographic refinement and atomic models of a human Fc fragment and its complex with fragment B of protein A from *Staphylococcus aureus* at 2.9- and 2.8-Å resolution. *Biochemistry* **20**, 2361-2370.
16. Derrick, J. P., and Wigley, D. B. (1992) Crystal structure of a streptococcal protein G domain bound to an Fab fragment. *Nature* **359**, 752-754.
17. Oda, M., Kozono, H., Morii, H., and Azuma, T. (2003) Evidence of allosteric conformational changes in the antibody constant region upon antigen binding. *Int. Immunol.* **15**, 417-426.

18. Schlessinger, J., Steinberg, I. Z., Givol, D., Hochman, J., and Pecht, I. (1975) Antigen-induced conformational changes in antibodies and their Fab fragments studied by circular polarization of fluorescence. *Proc. Natl. Acad. Sci. USA* **72**, 2775-2779.
19. Harris, L. J., Larson, S. B., and McPherson, A. (1999) Comparison of intact antibody structures and the implications for effector function. *Adv. Immunol.* **72**, 191-208.
20. Oi, V. T., Vuong, T. M., Hardy, R., Reidler, J., Dangle, J., Herzenberg, L. A., and Stryer, L. (1984) Correlation between segmental flexibility and effector function of antibodies. *Nature* **307**, 136-140.
21. Song, W., Cho, H., Cheng, P., and Pierce, S. K. (1995) Entry of B cell antigen receptor and antigen into class II peptide-loading compartment is independent of receptor cross-linking. *J. Immunol.* **155**, 4255-4263.
22. Batista, F. D., and Neuberger, M. S. (1997) Affinity dependence of the B cell response to antigen: a threshold, a ceiling, and the importance of off-rate. *Immunity* **8**, 751-759.
23. Azuma, T. (1997) Somatic hypermutation in mouse λ chains. *Immunol. Rev.* **162**, 97-105.
24. Torigoe, H., Nakayama, T., Imazato, M., Shimada, I., Arata, Y., and Sarai, A. (1995) The affinity maturation of anti-4-hydroxy-3-nitrophenylacetyl mouse monoclonal antibody. A calorimetric study of the antigen-antibody interaction. *J. Biol. Chem.* **270**, 22218-22222.
25. Furukawa, K., Akasako-Furukawa, A., Shirai, H., Nakamura, H., and Azuma, T. (1999) Junctional amino acids determine the maturation pathway of an antibody. *Immunity* **11**, 329-338.
26. Sagawa, T., Oda, M., Ishimura, M., Furukawa, K., and Azuma, T. (2003) Thermodynamics and kinetic aspects of antibody evolution during the immune response to hapten. *Mol. Immunol.* **39**, 801-808.
27. Burgen, A. S., Roberts, G. C., and Feeney, J. (1975) Binding of flexible ligands to macromolecules. *Nature* **253**, 753-755.
28. Foote, J., and Milstein, C. (1991) Kinetic maturation of an immune response. *Nature* **352**, 530-532.
29. Manivel, V., Sahoo, N. C., Salunke, D. M., and Rao, K. V. (2000) Maturation of an antibody response is governed by modulations in flexibility of the antigen-combining site. *Immunity* **13**, 611-620.
30. Liu, J., Liu, L., and Jemmerson, R. (2000) Immunoglobulin gene joints compensate for reduced on-rates imposed by somatic mutations in a V_H gene. *Mol. Immunol.* **37**, 95-105.
31. Jimenez, R., Salazar, G., Yin, J., Joo, T., and Romesberg, F. E. (2004) Protein dynamics and the immunological evolution of molecular recognition. *Proc. Natl. Acad. Sci. USA* **101**, 3803-3808.
32. Harris, L. J., Larson, S. B., Hasel, K. W., and McPherson, A. (1997) Refined structure of an intact IgG2a monoclonal antibody. *Biochemistry* **36**, 1581-1597.
33. Harris, L. J., Skaletsky, E., and McPherson, A. (1998) Crystallographic structure of an intact IgG1 monoclonal antibody. *J. Mol. Biol.* **275**, 861-872.
34. Mizutani, R., Miura, K., Nakayama, T., Shimada, I., Arata, Y., and Satow, Y. (1995) Three-dimensional structures of the Fab fragment of murine N1G9 antibody from the primary immune response and of its complex with (4-hydroxy-3-nitrophenyl)acetate. *J. Mol. Biol.* **254**, 208-222.
35. Guddat, L. W., Shan, L., Anchin, J. M., Linthicum, D. S., and Edmundson, A. B. (1994) Local and transmitted conformational changes on complexation of an anti-sweetener Fab. *J. Mol. Biol.* **236**, 247-274.
36. Wilson, I. A., and Stanfield, R. L. (1994) Antibody-antigen interactions: new structures and new conformational changes. *Curr. Opin. Struct. Biol.* **4**, 857-867.
37. Wedemayer, G. J., Patten, P. A., Wang, L. H., Schultz, P. G., and Stevens, R. C. (1997) Structural insights into the evolution of an antibody combining site. *Science* **276**, 1665-1669.
38. Yin, J., Beuscher, A. E. 4th, Andryski, S. E., Stevens, R. C., and Schultz, P. G. (2003) Structural plasticity and the evolution of antibody affinity and specificity. *J. Mol. Biol.* **330**, 651-656.
39. Chong, L. T., Duan, Y., Wang, L., Massova, I., and Kollman, P. A. (1999) Molecular dynamics and free-energy calculations applied to affinity maturation in antibody 48G7. *Proc. Natl. Acad. Sci. USA* **96**, 14330-14335.
40. Yin, J., Mundorff, E. C., Yang, P. L., Wendt, K. U., Hanway, D., Stevens, R. C., and Schultz, P. G. (2001) A comparative analysis of the immunological evolution of antibody 28B4. *Biochemistry* **40**, 10764-10773.
41. Dill, K. A., and Chan, H. S. (1997) From Levinthal to pathways to funnels. *Nat. Struct. Biol.* **4**, 10-19.
42. Ma, B., Kumar, S., Tsai, C. J., and Nussinov, R. (1999) Folding funnels and binding mechanisms. *Protein Eng.* **12**, 713-720.

43. Spolar, R. S., and Record, M. T. Jr. (1994) Coupling of local folding to site-specific binding of proteins to DNA. *Science* **263**, 777-784.
44. Oda, M., Furukawa, K., Ogata, K., Sarai, A., and Nakamura, H. (1998) Thermodynamics of specific and non-specific DNA binding by the c-Myb DNA-binding domain. *J. Mol. Biol.* **276**, 571-590.
45. Wright, P. E., and Dyson, H. J. (1999) Intrinsically unstructured proteins: re-assessing the protein structure-function paradigm. *J. Mol. Biol.* **293**, 321-331.
46. Tobita, T., Oda, M., Morii, H., Kuroda, M., Yoshino, A., Azuma, T., and Kozono, H. (2003) A role for the P1 anchor residue in the thermal stability of MHC class II molecule I-A^b. *Immunol. Lett.* **85**, 47-52.
47. Saito, K., Sarai, A., Oda, M., Azuma, T., and Kozono, H. (2003) Thermodynamic analysis of the increased stability of major histo-compatibility complex class II molecule I-E^k complexed with an antigenic peptide at an acidic pH. *J. Biol. Chem.* **278**, 14732-14738.
48. Saito, K., Oda, M., Sarai, A., Azuma, T., and Kozono, H. (2004) Contribution of a single hydrogen bond between βHis81 of MHC class II I-E^k and the bound peptide to the pH-dependent thermal stability. *Microbiol. Immunol.* **48**, 53-57.
49. Lee, A. L., and Wand, A. J. (2001) Microscopic origins of entropy, heat capacity and the glass transition in proteins. *Nature* **411**, 501-504.
50. Prabhu, N. V., Lee, A. L., Wand, A. J., and Sharp, K. A. (2003) Dynamics and entropy of a calmodulin-peptide complex studied by NMR and molecular dynamics. *Biochemistry* **42**, 562-570.
51. Wrabl, J. O., Shortle, D., and Woolf, T. B. (2000) Correlation between changes in nuclear magnetic resonance order parameters and conformational entropy: molecular dynamics simulations of native and denatured staphy-lococcal nuclease. *Proteins* **38**, 123-133.
52. Smith, T. J., Olson, N. H., Cheng, R. H., Chase, E. S., and Baker, T. S. (1993) Structure of a human rhinovirus-bivalently bound antibody complex: implications for viral neutralization and antibody flexibility. *Proc. Natl. Acad. Sci. USA* **90**, 7015-7018.
53. Hewat, E. A., and Blaas, D. (1996) Structure of a neutralizing antibody bound bivalently to human rhinovirus 2. *EMBO J.* **15**, 1515-1523.
54. Akasaka, K. (2003) Highly fluctuating protein structures revealed by variable-pressure nuclear magnetic resonance. *Biochemistry* **42**, 10875-10885.
55. James, L. C., Roversi, P., and Tawfik, D. S. (2003) Antibody multispecificity mediated by conformational diversity. *Science* **299**, 1362-1367.
56. Jimenez, R., Salazar, G., Baldridge, K. K., and Romesberg, F. E. (2003) Flexibility and molecular recognition in the immune system. *Proc. Natl. Acad. Sci. USA* **100**, 92-97.
57. Carlson, H. A. (2002) Protein flexibility and drug design: how to hit a moving target. *Curr. Opin. Chem. Biol.* **6**, 447-452.
58. Landolfi, N. F., Thakur, A. B., Fu, H., Vasquez, M., Queen, C., and Tsurushita, N. (2001) The integrity of the ball-and-socket joint between V and C domains is essential for complete activity of a humanized antibody. *J. Immunol.* **166**, 1748-1754.
59. Khalifa, M. B., Weidenhaupt, M., Choulier, L., Chatellier, J., Rauffer-Bruyere, N., Altschuh, D., and Vernet, T. (2000) Effects on interaction kinetics of mutations at the VH-VL interface of Fabs depend on the structural context. *J. Mol. Recognit.* **13**, 127-139.
60. Aburatani, T., Ueda, H., and Nagamune, T. (2002) Importance of a CDR H3 basal residue in V_H/V_L interaction of human antibodies. *J. Biochem. (Tokyo)* **132**, 775-782.
61. Stein, P. E., Leslie, A. G., Finch, J. T., and Carrell, R. W. (1991) Crystal structure of uncleaved ovalbumin at 1.95 Å resolution. *J. Mol. Biol.* **221**, 941-959.
62. Motoshima, H., Mine, S., Masumoto, K., Abe, Y., Iwashita, H., Hashimoto, Y., Chijiiwa, Y., Ueda, T., and Imoto, T. (1997) Analysis of the stabilization of hen lysozyme by helix macrodipole and charged side chain interaction. *J. Biochem. (Tokyo)* **121**, 1076-1081.
63. Bhattacharya, A. A., Curry, S., and Franks, N. P. (2000) Binding of the general anesthetics propofol and halothane to human serum albumin. High resolution crystal structures. *J. Biol. Chem.* **275**, 38731-38738.

Communicated by Hiroshi Ueno